

# Jost-matrix analysis of experimental data on $d^4\text{He}$ scattering

P. Vaandrager\*, S.A. Rakityansky†

Dept. of Physics, University of Pretoria, Pretoria, South Africa

January 2, 2020

## Abstract

Two sets of data for  $d\alpha$  scattering are analysed to determine the parameters of the bound and resonant states of the nuclear system  ${}^6\text{Li}$  with quantum numbers  $1^+$ ,  $2^+$ ,  $3^+$ ,  $2^-$ , and  $3^-$ , as well as to find the corresponding  $S$ -matrix residues. These data ( $d\alpha$  cross-sections) are fitted by both a single-channel and a two-channel  $S$ -matrix that is written in terms of semi-analytic Jost matrices, where all the factors, responsible for the branching of the energy Riemann surface, are given explicitly and exactly while the remaining unknown functions are represented by power series with the coefficients being the fitting parameters. The Jost matrices obtained from the fitting, are used at complex energies to locate resonances and the bound state, as well as to determine the corresponding  $S$ -matrix residues and the Asymptotic Normalization Coefficients (ANC). Our analysis, based on an  $S$ -matrix with the correct analytic structure, gives a solid confirmation of the resonance parameters found by the other authors.

**Keywords** Jost matrices, Coulomb interaction, resonances, bound state,  $S$ -matrix residues, Asymptotic Normalization Coefficient,  ${}^6\text{Li}$

## 1 Introduction

The nucleus  ${}^6\text{Li}$  belongs to the group of the lightest nuclides that have a rather simple spectrum, consisting of less than a dozen well distinguished levels [1]. The abundance of this

---

\*e-mail: paul.vaandrager@up.ac.za

†e-mail: rakitsa@up.ac.za

isotope is very small ( $\sim 7.6\%$ ) as compared to that of  ${}^7\text{Li}$  ( $\sim 92.4\%$ ), but its importance in thermonuclear  $dt$ -fusion motivated many researchers to study  ${}^6\text{Li}$  both theoretically and experimentally. In the  $dt$ -fusion, the nucleus  ${}^6\text{Li}$  serves as a stable “storage” of tritium that can be released by the neutron “ignition”  $n + {}^6\text{Li} \rightarrow t + \alpha$ .

The nucleus  ${}^6\text{Li}$  is also of importance in astrophysics, especially in connection with the puzzle associated with its abundance. It is believed that its synthesis via the radiative capture  $\alpha(d, \gamma){}^6\text{Li}$  was the main process by which the isotope  ${}^6\text{Li}$  was produced during the primordial nucleosynthesis as well as subsequently in stars [2]. However, the observed abundance of  ${}^6\text{Li}$  does not agree with the predictions of the *Big Bang Theory* [3], which is known as the *Lithium Discrepancy*.

Many collision processes, and in particular the radiative capture  $\alpha(d, \gamma){}^6\text{Li}$ , may go via the intermediate formation of resonances. This is one of the reasons why the accurate knowledge of the parameters of these resonances is needed. Among these important parameters are the Asymptotic Normalization Coefficients (ANC) that determine the behaviour of the resonance wave functions at large distances, where the radiative capture mainly happens because of the Coulomb repulsion between the colliding nuclei. So far, the ANC are found only for several among many known excited states of  ${}^6\text{Li}$  (see, for example, Ref. [4]). One of our aims was to partly cover this gap and to confirm the values or to improve the accuracy of the known parameters.

In its ground state the nucleus  ${}^6\text{Li}$  can be viewed as a bound state of the  $\alpha$ -particle and deuteron [5]. The  $\alpha$ -particle is the most tightly bound nuclear complex and therefore a configuration with the presence of such a cluster should remain dominant at the excitation energies at least up to  $\sim 20$  MeV. In contrast to that, the deuteron cluster “dissolves” and becomes the  $pn$  pair at much lower energies. This means that in a theoretical consideration of the excited states of  ${}^6\text{Li}$  one has to deal with at least the three-body system,  $\alpha pn$ .

However, when analysing experimental scattering data, we only look at the initial and final channels. The constituents of the intermediate collision complex is something of a “black box” for us. If we manage to construct an  $S$ -matrix that correctly describes the observed transitions among the channels, then it does not matter what kind of configurations are formed in that “box”. The poles of such an  $S$ -matrix should be at the correct (complex) resonance energies. Of course, such an  $S$ -matrix will not reproduce all possible resonances, but only those that are reachable from the channels taken into account.

In our present analysis, we only consider the data on the elastic  $d\alpha$  scattering. Since the isospins of both  $d$  and  $\alpha$  are zero, we can only find the resonances with zero total isospin (although in the spectrum of  ${}^6\text{Li}$  there are states with  $T = 1$  [1]). In fact, most of the low-lying levels of this nucleus have isospin zero and decay into the  $d\alpha$  channel. This makes our analysis reasonable and substantiated.

$J^\pi$	coupled $d\alpha$ -channels
$0^-$	$P_0$
$1^+$	$S_1 - D_1$
$1^-$	$P_1$
$2^+$	$D_2$
$2^-$	$P_2 - F_2$
$3^+$	$D_3 - G_3$
$3^-$	$F_3$
$4^-$	$F_4 - H_4$

Table 1: Coupled partial waves in the  $d\alpha$ -collision for several lowest values of the total angular momentum  $J$ .

## 2 Multi-channel $S$ -matrix

All the channels we consider may only differ by the orbital angular momentum  $\ell$  (different partial waves), i.e. they have the same thresholds and therefore are degenerate in the energy. Since the spins of deuteron and the  $\alpha$ -particle are 1 and 0, and since the parity,  $\pi$ , is conserving, the maximum number of coupled partial waves for a given total angular momentum  $J$  is two. The channels we consider are given in Table 1.

For each state with definite  $J^\pi$ , the  $S$ -matrix at the energy  $E$  can be written in terms of the corresponding Jost matrices (see, for example, Ref. [6]),

$$S(E) = f^{(\text{out})}(E) [f^{(\text{in})}(E)]^{-1} , \quad (1)$$

where we drop the symbols  $J$  and  $\pi$ . For the Jost matrices in the above equation, we use the exact semi-analytic expressions obtained in Ref. [6],

$$f_{\ell'\ell}^{(\text{in/out})}(E) = \frac{e^{\pi\eta/2}\ell'!}{\Gamma(\ell'+1 \pm i\eta)} \left\{ \frac{C_\ell(\eta)k^{\ell-\ell'}}{C_{\ell'}(\eta)} A_{\ell'\ell}(E) - \left[ \frac{2\eta h(\eta)}{C_0^2(\eta)} \pm i \right] C_{\ell'}(\eta) C_\ell(\eta) k^{\ell'+\ell+1} B_{\ell'\ell}(E) \right\} , \quad (2)$$

where  $k$  is the wave number (common for all the channels with the same thresholds and the

same reduced mass  $\mu$ ),

$$k = \pm \sqrt{2\mu E/\hbar^2} , \quad (3)$$

$C_\ell(\eta)$  is the Coulomb barrier factor depending on the Sommerfeld parameter  $\eta$ ,

$$C_\ell(\eta) = \frac{2^\ell e^{-\pi\eta/2}}{(2\ell)!!} \exp \left\{ \frac{1}{2} [\ln \Gamma(\ell + 1 + i\eta) + \ln \Gamma(\ell + 1 - i\eta)] \right\} \xrightarrow{\eta \rightarrow 0} 1 , \quad (4)$$

and

$$h(\eta) = \frac{1}{2} [\psi(i\eta) + \psi(-i\eta)] - \ln \eta , \quad \psi(z) = \frac{\Gamma'(z)}{\Gamma(z)} , \quad \eta = \frac{e^2 Z_1 Z_2 \mu}{\hbar^2 k} . \quad (5)$$

The matrices  $A$  and  $B$  in Eq. (2) are unknown. They are determined by the dynamics of the physical system.

As is seen, the Jost matrices (and thus the  $S$ -matrix) are not single-valued functions of the variable  $E$ . This is due to the two reasons. Firstly, for a given energy there are two possibilities for obtaining the wave number: by choosing the sign in front of the square root (3). Secondly, the function  $h(\eta)$  involves  $\ln(k)$ , which assumes an infinite number of different values for a complex  $k$ . Therefore, for a single value of  $E$  there are infinitely many values of  $S(E)$ . As a result, the  $S$ -matrix is defined on a Riemann surface with spiral topology, where the threshold,  $E = 0$ , is the branch point of the square-root and the logarithm type at the same time (see, Refs. [7, 8]).

In Ref. [6] it is shown that the matrices  $A$  and  $B$  in the semi-analytic representations (2) are single-valued analytic functions of  $E$ , i.e. they are defined on a simple complex plane without any branch points. These matrices are the same on all the sheets of the Riemann surface. All the troubles with the branching of the Riemann surface are caused by the explicit factors in (2). It should be emphasized that these representations are exact (rigorously derived from the multi-channel Schrödinger equation) and are valid for any physical system with binary channels. In simple words, the explicit factors in them are the same for any such system (they, kind of, describe the kinematics), while the unknown single-valued matrices  $A$  and  $B$  describe the specific dynamics.

Since the matrices  $A$  and  $B$  are single-valued and analytic, we can use any reasonable approximation for them. Such an approximation does not affect the analytic structure of the  $S$ -matrix, i.e. the topology of its Riemann surface and the symmetry relations among the values of the  $S$ -matrix at different points on this surface. Keeping the correct analytic structure is important when the  $S$ -matrix is analytically continued from the real axis to complex energies for the purpose of locating possible resonances. Such an analytic continuation is very often used, when the  $S$ -matrix is (approximately) constructed by fitting the scattering data.

In the present work, we also fit the data (cross sections). In doing this, we choose a point  $E_0$  on the real axis somewhere in the middle of the energy interval, where the data points are

available, and approximate the matrices  $A$  and  $B$  by several terms of their Taylor expansions around  $E_0$ ,

$$A(E) \approx a^{(0)} + a^{(1)}(E - E_0) + a^{(2)}(E - E_0)^2 + \dots + a^{(M)}(E - E_0)^M, \quad (6)$$

$$B(E) \approx b^{(0)} + b^{(1)}(E - E_0) + b^{(2)}(E - E_0)^2 + \dots + b^{(M)}(E - E_0)^M, \quad (7)$$

where the unknown expansion coefficients (elements of the matrices  $a$  and  $b$ ) serve as the fitting parameters.

After finding the optimal values of these parameters, we obtain a reliable approximation for the  $S$ -matrix (1), which has the correct analytic properties. Then the resonances can be found as the roots of the equation

$$\det f^{(\text{in})}(E) = 0 \quad (8)$$

on the corresponding non-physical sheet of the Riemann surface. Choice of the appropriate sheet is done by choosing the sign in Eq. (3) and taking the principal branch of the logarithmic function  $\ln(k)$ .

Since all the poles of the  $S$ -matrix are simple, its residues at these poles can be found by numerical differentiation of the determinant of the Jost matrix  $f^{(\text{in})}(E)$  in Eq. (1), as described in Ref. [8]. Such a residue of a diagonal element of the  $S$ -matrix determines the asymptotic normalization coefficient  $\mathcal{A}_\ell$  of the wave function. The derivation of the corresponding relation can be found in Ref. [9]. This relation involves an arbitrary factor whose choice is a matter of convention (depends on the definition of  $\mathcal{A}_\ell$ ). In order to compare our results with the previous calculations, we use here the relation

$$\text{Res}[S_{\ell\ell}, E] = i(-1)^{\ell+1} \frac{\hbar^2 k}{\mu} e^{-\pi\eta} \mathcal{A}_\ell^2, \quad (9)$$

which is equivalent to the relevant formulae of Ref. [4].

### 3 Experimental data and fitting procedure

As the  $d\alpha$ -data for our fitting, we take and combine two different sets of scattering cross-sections, denoted further as the sets A and B. They cover adjacent intervals of the collision energy and thus complement each other.

**Data set A** consists of the  $d\alpha$  cross sections obtained from the corresponding phase-shifts of Ref. [10], where it was done an energy independent analysis of 3900 raw experimental data

points with channel coupling included. These phase-shifts cover the C.M. energy range from 4 MeV to 30 MeV. There are roughly 20 data points available for each of the partial waves with  $\ell = 0, 1, 2, 3, 4, 5$ .

**Data set B** is made of the  $d\alpha$  cross sections, which we derived from the Padé approximation of the  $S$ -matrix that was obtained in Ref. [11] by fitting energy-dependent single-channel experimental data in the the C.M. energy interval from 0.5 MeV to 3.5 MeV. Channel coupling was not taken into account by the authors of Ref. [11]. Since their  $S$ -matrix is given in an explicit form, we can generate from it a sequence of data points convenient for our analysis, even outside the original energy-interval. Using this freedom, we generated 40 points in each channel that evenly cover the C.M. energies from 0.4 MeV to 4.0 MeV.

Therefore, combining the sets A and B, we have (for each channel) 40 points between 0.4 MeV and 4 MeV, and 20 points between 4 MeV and 30 MeV. The sets A and B are consistent, i.e. they rather smoothly match at around 4 MeV. Actually, the same data were used in Ref. [4], where a method, similar to the effective-range expansion, was applied for extracting the information about the discrete states of the  $d\alpha$ -system. In doing this, the authors of Ref. [4] analysed the data sets A and B separately. We, however, following the suggestion of Ref. [11], chose to combine the two sets and treated them as a single one.

In the present work, we use the same fitting procedure as was described in Refs. [7–9, 12]. In short, for each available data point,  $\sigma_\ell^{\text{exp}}(E)$ , we calculate the corresponding fitting cross section

$$\sigma_\ell^{\text{fit}}(E) = \frac{\pi(2J+1)}{3k^2} |S_{\ell\ell}(E) - 1|^2, \quad (10)$$

which depends on the fitting parameters  $a^{(n)}$  and  $b^{(n)}$  used in the expansions (6, 7), and minimize the function

$$\chi^2 = \sum_{i=1}^{N_1} [\sigma_{\ell_1}^{\text{exp}}(E_i) - \sigma_{\ell_1}^{\text{fit}}(E_i)]^2 + \sum_{i=1}^{N_2} [\sigma_{\ell_2}^{\text{exp}}(E_i) - \sigma_{\ell_2}^{\text{fit}}(E_i)]^2. \quad (11)$$

Here the first sum takes into account the deviations of the fitted points from the experimental ones in the first channel, and the second sum runs over the data points in the second channel (if it exists for a given  $J$ , as shown in Table 1).  $N_1$  and  $N_2$  are the numbers of the data points taken into account in the first and the second channels, respectively. The minimization was done using the code MINUIT [13].

It should be noted that any diagonal matrix element  $S_{\ell\ell}$  obtained as the “ratio” (1), depends on all the elements of the matrix  $f^{(\text{in})}$  (diagonal and off-diagonal), i.e. on all the elements of the parameter matrices  $a^{(n)}$  and  $b^{(n)}$ . This means that coupling of the channels is always present in our fitting procedure, and it is taken into account in the correct way. Even

$E_r$ [MeV]	$\Gamma$ [MeV]	Res[ $S_{00}, E$ ] [MeV]	Res[ $S_{22}, E$ ] [MeV]	$ \mathcal{A}_0 $ [fm <sup>1/2</sup> ]	$ \mathcal{A}_2 $ [fm <sup>1/2</sup> ]	Ref.
-1.4691		29.588	0.00603	2.3330	0.0252	this work
		+i42.904	-i0.00079	1.960	0.093	[4] (v. 1)
				1.900	0.025	[4] (v. 2)
-1.4743						[1] (accepted)
3.8858	2.6324	0.00196	-1.7743	0.0153	0.4768	this work
		+i0.00087	-i1.0906			
3.900	2.347			0.028	0.455	[4] (v. 1)
3.872	1.860			0.018	0.392	[4] (v. 2)
4.18 ± 0.05	1.5 ± 0.2					[1] (accepted)

Table 2: Parameters of the bound and resonant states of  ${}^6\text{Li}$  with  $J^\pi = 1^+$ , obtained from a two-channel fit of the elastic cross sections for the  $S_1$  and  $D_1$  partial waves of the  $d$ - $\alpha$  scattering. The corresponding parameters from Refs. [1, 4] are given here for the purpose of comparison.

if we were fitting only one channel (when the second one exists) all the fitting parameters are involved in such a fit, and thus the resulting  $S$ -matrix should correctly describe the second one as well. Such a “predictive” power of our procedure was previously demonstrated in some model problems (see Refs. [12, 14]).

## 4 Results

When fitting the data, we used several different central points  $E_0$  and different numbers  $M$  in the expansions (6, 7). The choice of these parameters was determined by the choice of the energy domain where we were looking for a resonance. It is obvious that the closer  $E_0$  is to the resonance point, the more accurately it can be located. By repeating the calculations for the same resonance with different  $E_0$  or  $M$  we can check the accuracy achieved. Indeed, ideally, the resonance parameters should not depend on such a choice. Therefore all the digits in their values that remain the same with different  $E_0$ , for example, can be considered as accurate.

Speaking about the particular channels, we begin with the coupled  $S_1$  and  $D_1$  partial waves in the state  $1^+$ . The results of our analysis for them are given in Table 2. The corresponding fit was done with  $E_0 = -1.45$  MeV and  $M = 1$ . The quality of the fit can be seen in Figs. 1 and 2. The bound state energy we obtained, agrees well with the value that is considered as accepted in the compilation [1]. Our ANC for the  $S_1$  partial wave is somewhat larger than the values from Ref. [4]. Our ANC for the  $D_1$  partial wave agrees with one of the two values reported in Ref. [4], where it was supposed that the  $S_1 - D_1$  coupling was weak, since the  $D_1$ -ANC was small as compared to  $S_1$ -ANC. However, the comparison of these values is not a decisive argument for such a conclusion. A reasonable judgement about the strength of the coupling between any two channels can be done, if the cross section of the transition between them is considered. As we mention at the end of Sec. 3, our method has an advantage that the same fitting parameters describe all the elastic and inelastic processes. Therefore, after fitting the  $S_1$  and  $D_1$  channels, we automatically obtain the correct transition cross-section, which is shown in Fig. 3. As is seen, it is three orders of magnitude smaller than both the elastic cross sections, shown in Figs. 1 and 2. This means that the  $S_1 - D_1$  coupling is weak indeed.

As far as the  $1^+$  resonance in the coupled  $S_1 - D_1$  channels is concerned, our results agree well with those from Ref. [4]. This can be said not only about the resonance energy and width, but also about the ANC values. However our width is somewhat larger than the value accepted in the compilation [1]. The weak coupling between the two partial waves results in the absence of any visible irregularities around the resonance energy,  $E \sim 3.9$  MeV, in the  $S_1$  cross section. The  $1^+$  resonance at this energy is completely dominated by the  $D_1$  wave. A possible explanation can be that a potential barrier is needed to sustain this resonance, and in the state with  $\ell = 2$  there is the centrifugal barrier for that purpose. After this resonance is formed in the  $D_1$  wave, it can decay back to the same wave or to the  $S_1$  wave. However, because of the weak coupling between them, the probability of decaying into the  $S_1$  wave is very small. Nonetheless, it is nonzero and contributes something to the total width. This is why our total width is a bit greater than that of Ref. [4], where the coupling was completely ignored.

The next state that we consider is the partial wave  $D_2$  ( $J^\pi = 2^+$ ), which is not coupled to any other waves. The data points for this state and the corresponding cross section from the fitting with  $E_0 = 2.6$  MeV and  $M = 3$ , are shown in Fig. 4. In this channel, we found one resonance at the energy  $E = (2.8448 - \frac{i}{2}1.3229)$  MeV, which practically coincides with the value accepted in the compilation [1]. The  $S$ -matrix residue and the corresponding ANC are given in Table 3.

Next in the list are two quantum states  $2^-(P_2 - F_2)$  and  $3^+(D_3 - G_3)$  that are both mixtures of two partial waves. However, similar to the ( $S_1 - D_1$ ) case, we found that the



$J^\pi$	$\ell_J$	$E_r$ [MeV]	$\Gamma$ [MeV]	$\text{Res}[S_\ell, E_r - \frac{i}{2}\Gamma]$ [MeV]	$ \mathcal{A}_\ell $ [fm <sup>1/2</sup> ]	Ref.
2 <sup>+</sup>	$D_2$	2.8448	1.3229	$-1.0387 - i0.7135$	0.4262	this work
		2.960	0.995		0.349	[4] (set A fit)
		2.802	1.178		0.384	[4] (set B fit)
		$2.838 \pm 0.022$	$1.30 \pm 0.1$			[1] (accepted)
3 <sup>+</sup>	$D_3$	0.7135	0.0219	$0.0141 - i0.0166$	0.1124	this work
		0.690	0.024		0.119	[4] (set A fit)
		0.704	0.025		0.121	[4] (set B fit)
		$0.712 \pm 0.002$	$0.024 \pm 0.002$			[1] (accepted)
3 <sup>+</sup>	$D_3$	9.1632	8.2023	$0.7411 - i1.1532$	0.2793	this work
		14.326	17.8			[10]
2 <sup>-</sup>	$F_2$	20.906	29.034	$-20.743 - i0.8508$	0.8043	this work
		25.526	22			[10] (Sol. A)
		19.526	30			[10] (Sol. C)
3 <sup>-</sup>	$F_3$	10.305	16.724	$-7.3697 + i4.7254$	0.5403	this work
		22.526	16			[10]

Table 3: Parameters of <sup>6</sup>Li resonances in the states with 2<sup>+</sup>, 3<sup>+</sup>, 2<sup>-</sup>, and 3<sup>-</sup> obtained from fitting of the corresponding cross sections of the  $d\alpha$  scattering. The available values of the corresponding parameters from Refs. [1, 4, 10].

cross sections for the transitions  $P_2 \leftrightarrow F_2$  and  $D_3 \leftrightarrow G_3$  are several orders of magnitude smaller than the corresponding elastic cross sections. This implies that the couplings in these pairs of partial waves are extremely weak and therefore the resonances (if any) are dominated by a single wave in both states. We tried both the two-channel fits for the pairs  $(P_2 - F_2)$ ,  $(D_3 - G_3)$  and the single channel fits for each of the waves  $P_2$ ,  $F_2$ ,  $D_3$ , and  $G_3$  separately. The single channel fits reveal resonances only in the waves  $F_2$  and  $D_3$ . The two-channel fits give the  $2^-$  and  $3^+$  resonances with the same parameters as were obtained via the single-channel fits. In this way, we found one resonance in the state  $2^-$  and two resonances in the state  $3^+$ . Their parameters are given in Table 3, where only the dominant partial waves are shown. The corresponding fits of the cross sections are shown in Figs. 5 and 6. They were done with  $E_0 = 1.0$  MeV and  $M = 5$  for  $D_3$  and with  $E_0 = 30$  MeV and  $M = 2$  for  $F_2$ .

The last resonance that we found, is in the state  $3^-(F_3)$ , which involves only one partial wave. Its parameters are also shown in Table 3. The cross section for this state together with the fitted curve ( $E_0 = 15$  MeV,  $M = 2$ ) are shown in Fig. 7.

It should be noted that the resonances that we found in the partial waves  $F_2$ ,  $F_3$ , and the second resonance in  $D_3$ , were not included in the accepted list of Ref. [1]. They are very wide and are therefore difficult to find with any method. The only work where the resonances in these states were reported was the old paper [10]. As is seen from Table 3, our findings only roughly put these resonance points in the same places. This means that an independent confirmation is needed before they can be considered as firmly established. It is seen from Figs. 5 and 7 that there is much experimental uncertainty in the available data for the partial waves  $F_2$  and  $F_3$  and therefore deducing reliable resonance parameters for these channels is difficult.

In our initial fitting attempts, where the data sets A and B were considered separately, vastly different results were obtained, indicating the importance of using a larger energy range in performing fittings to obtain parameters for wide resonances.

Lastly, we should say that no resonances were found (as was expected) in the other states listed in Table 1.

Speaking in general, our calculations reasonably reproduce (confirm) the parameters of the bound state of  ${}^6\text{Li}$  as well as the parameters of all the resonances with isospin zero given in Ref. [1]. We also approximately confirmed some of the resonances not included in the compilation [1], but found in Ref. [10]. Since we are able to check the accuracy of our results, we may claim that the parameters we publish here, are reliable in the sense that they most accurately correspond to the data from which they were deduced.

## Acknowledgements

We are grateful to the National Research Foundation (NRF) of South Africa for making this study possible.

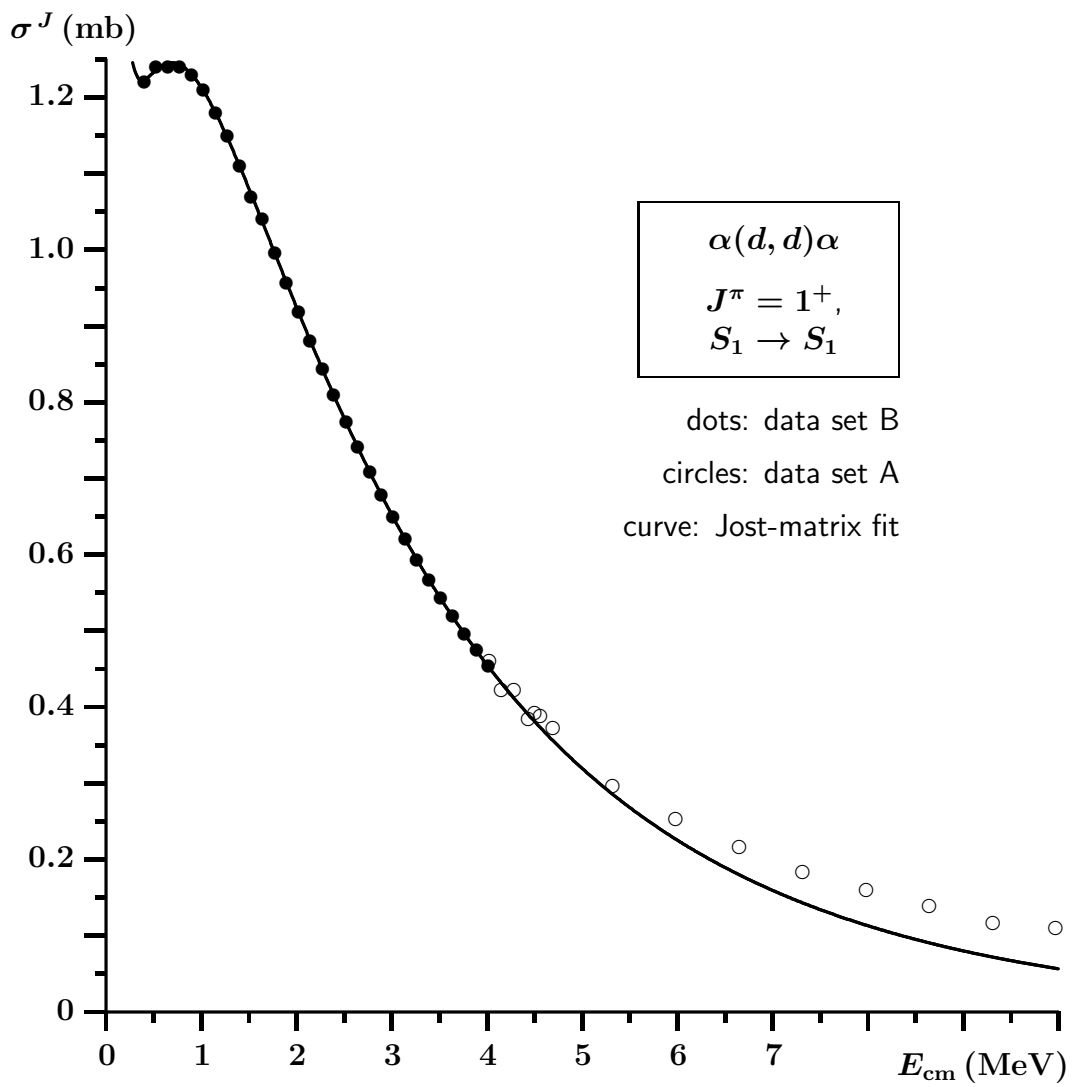


Figure 1: Fit of the data points in the partial wave  $S_1$ .

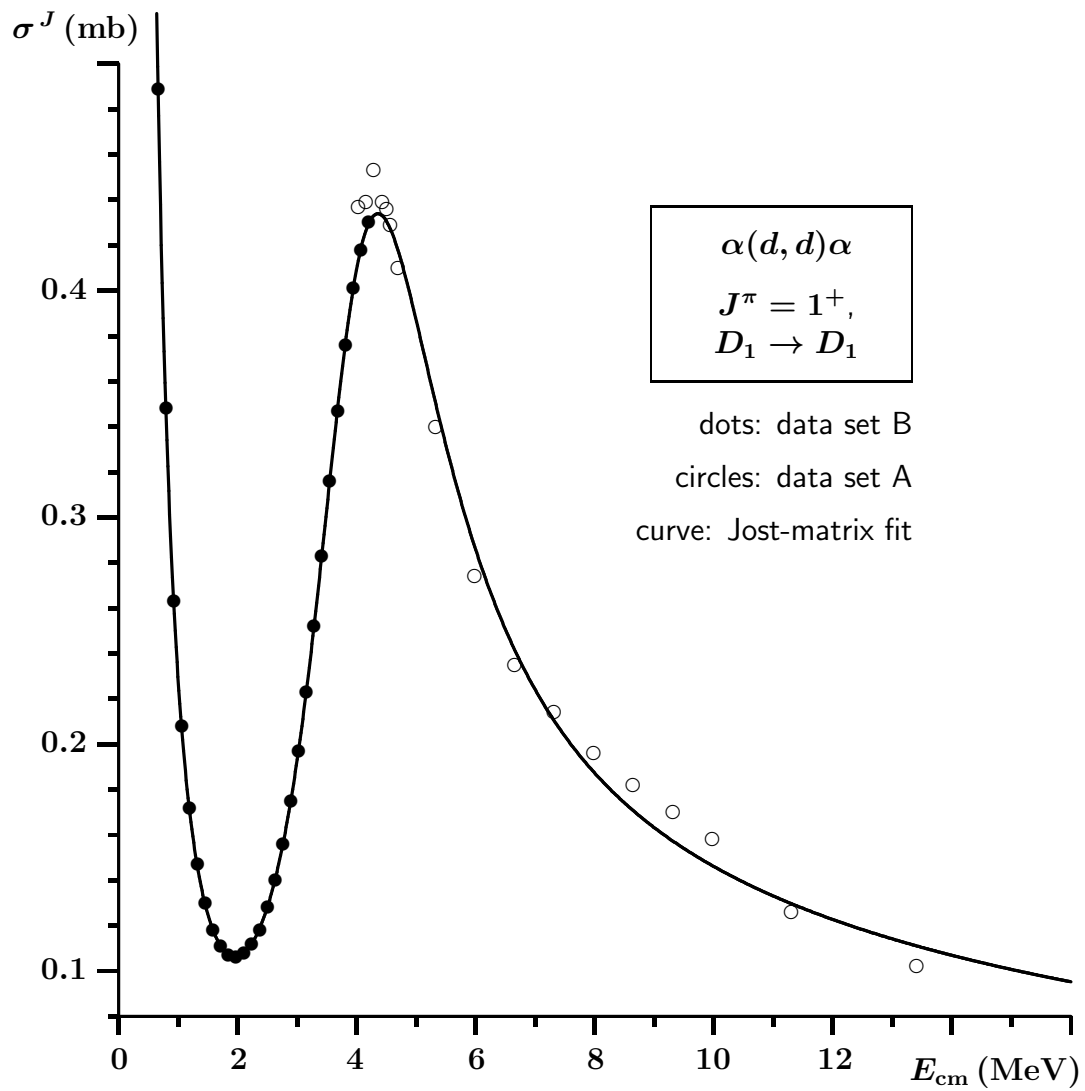


Figure 2: Fit of the data points in the partial wave  $D_1$ .

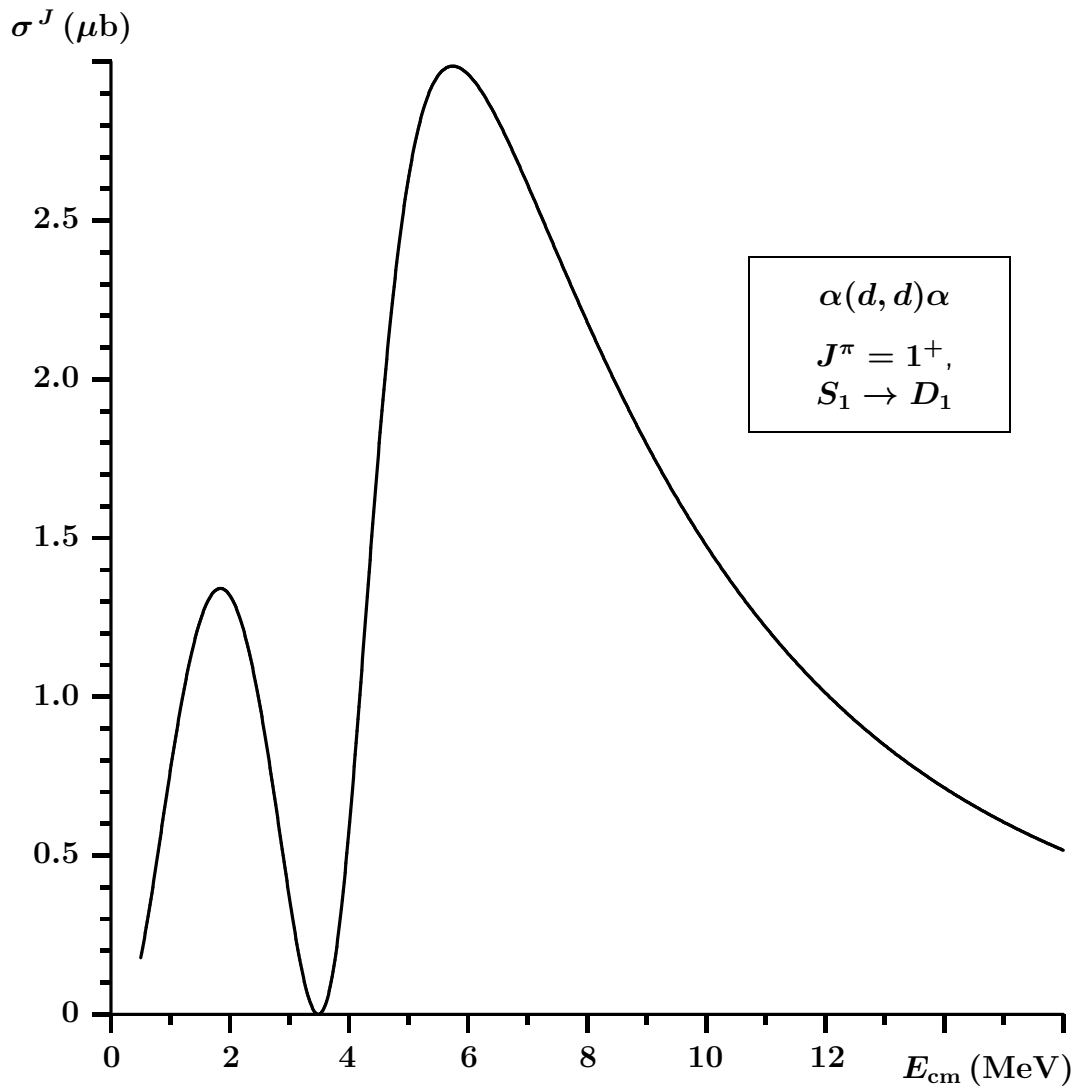


Figure 3: Cross section for the transition between the partial waves  $S_1$  and  $D_1$ .

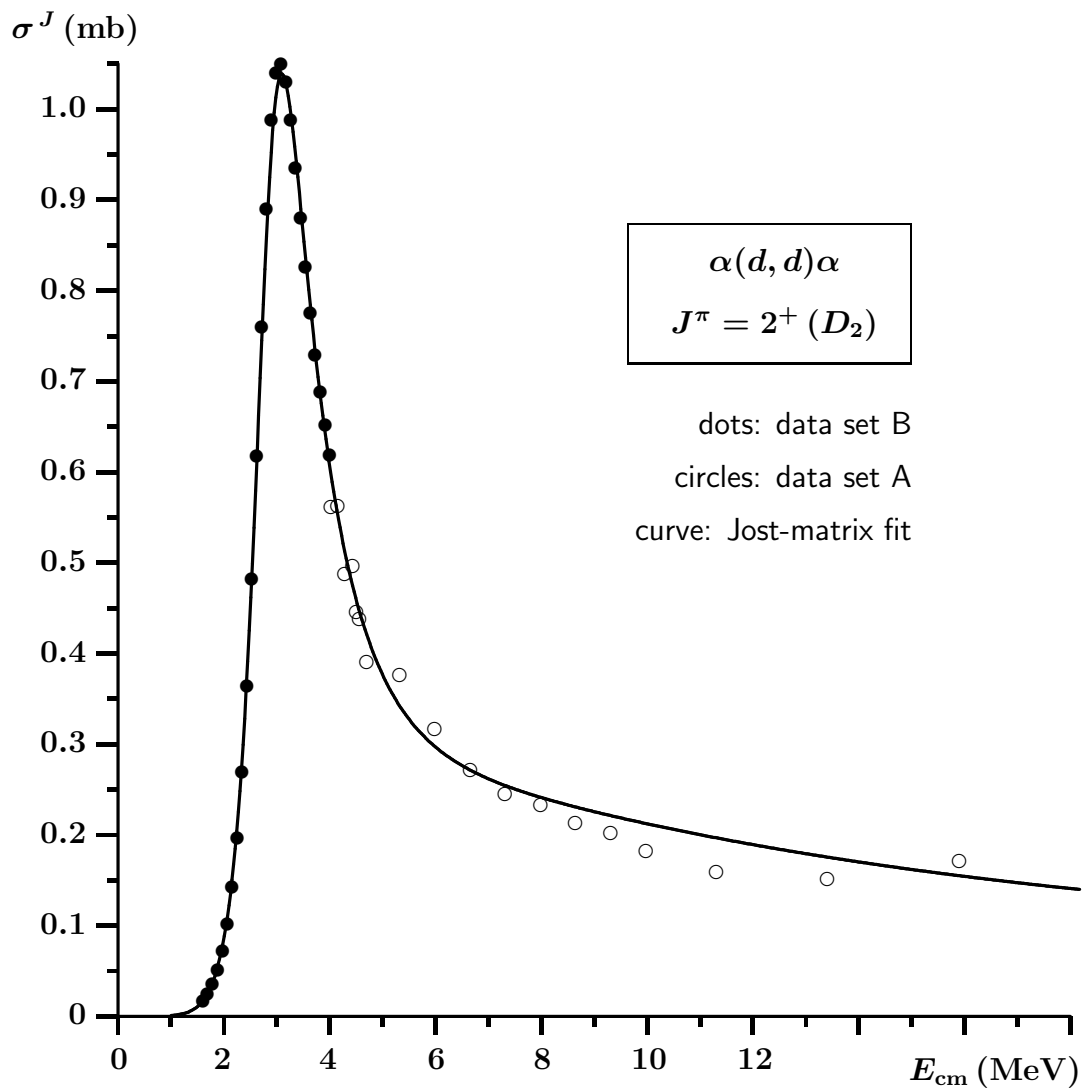


Figure 4: Fit of the data points in the partial wave  $D_2$ .

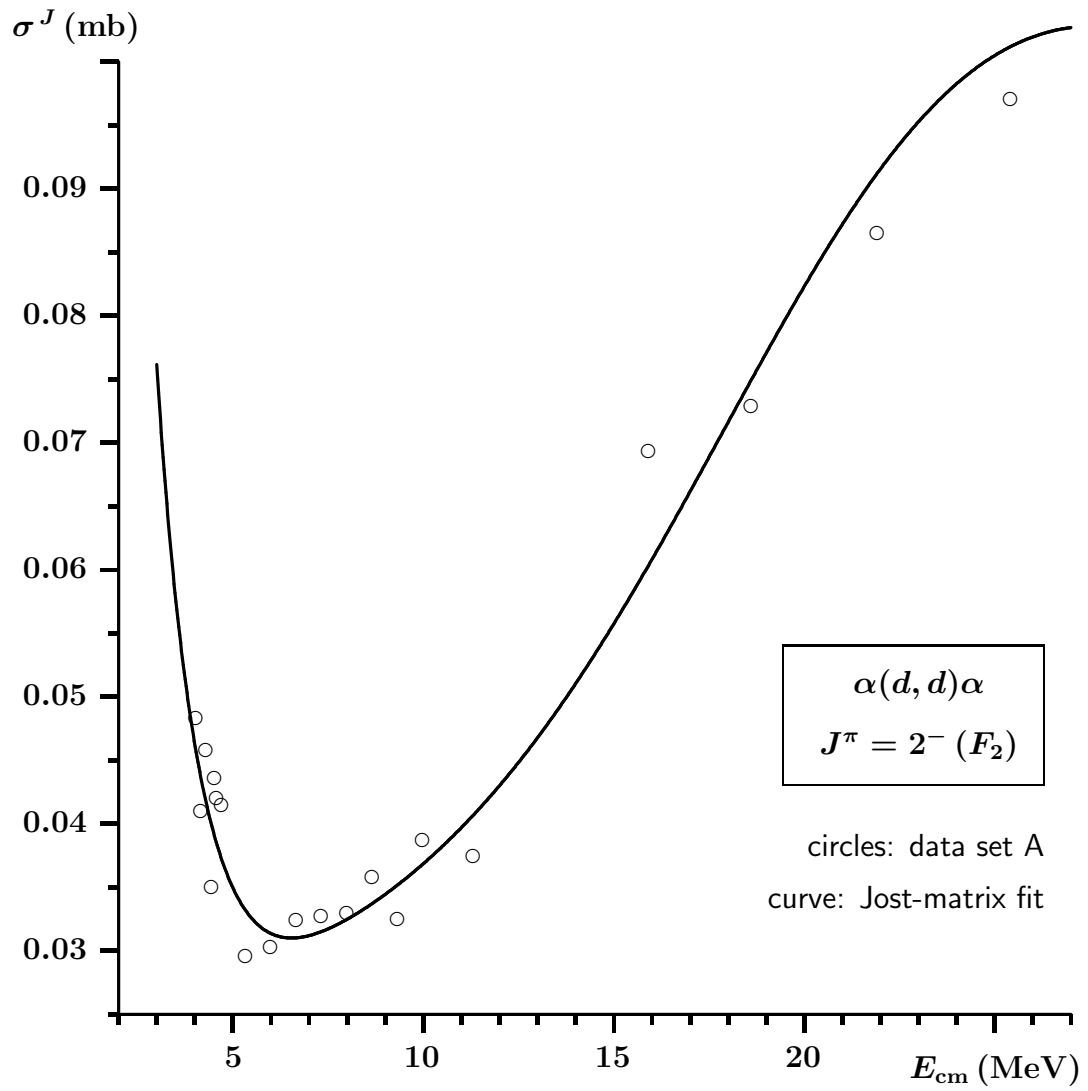


Figure 5: Fit of the data points in the partial wave  $F_2$ .



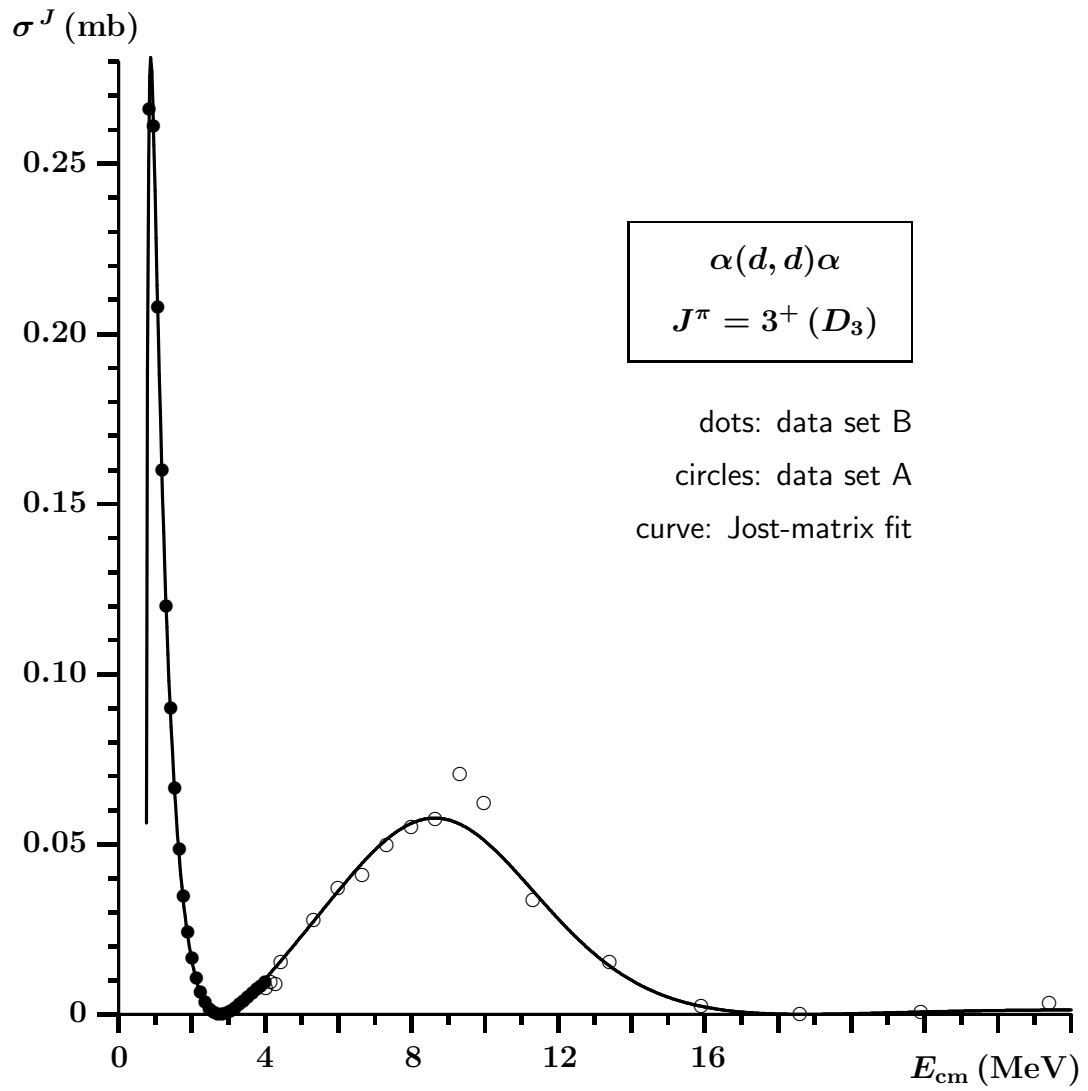


Figure 6: Fit of the data points in the partial wave  $D_3$ .

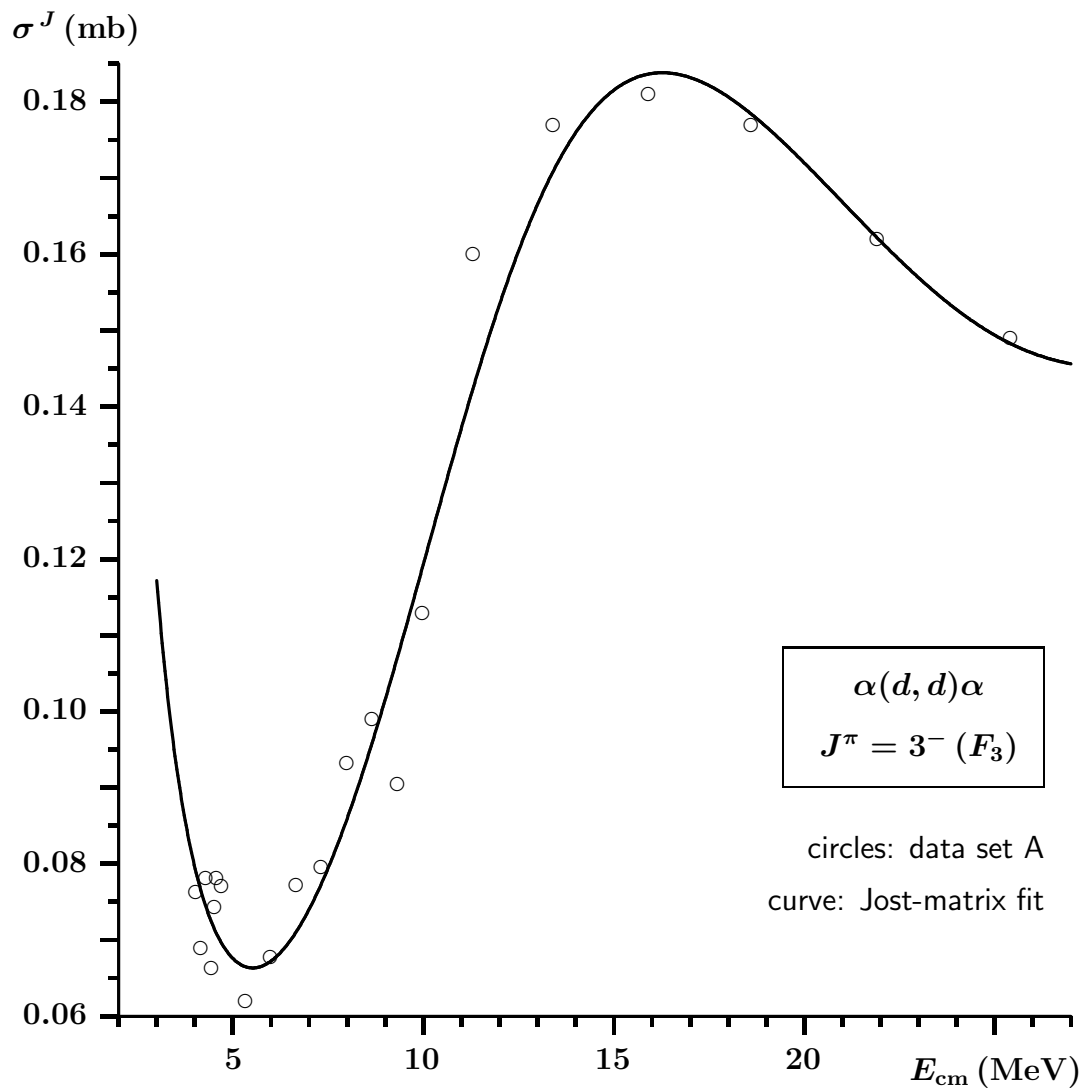


Figure 7: Fit of the data points in the partial wave  $F_3$ .

## References

- [1] D.R. Tilley, C.M. Cheves, J.L. Goldwin, G.M. Hale, H.M. Hofmann, J.H. Kelley, C.G. Sheu, H.R. Weller, "Energy levels of light nuclei  $A = 5, 6, 7$ ", Nucl. Phys. A **708**, pp. 3-163 (2002)
- [2] F.E. Cecil, J.S. Yan, C.S. Galovich, "The reaction  $d(\alpha, \gamma)^6\text{Li}$  at low energies and the primordial nucleosynthesis of  $^6\text{Li}$ ", Phys. Rev. C **53**(4), pp. 1967-1970, 1996
- [3] D. N. Schramm, R. V. Wagoner, "Element Production in the Early Universe", Annu. Rev. Nucl. Sci. **27**, pp. 37-74 (1977)
- [4] L. D. Blokhintsev, L. I. Nikitina, Yu. V. Orlov, D. A. Savin, "Characteristics of  $d + \alpha$  Bound and Resonant States from Analytic Continuation of the Effective-Range Expansion", Few-Body Syst. **55**, pp. 1009-2012 (2013)
- [5] S. Satsuka and W. Horiuchi, "Emergence of nuclear clustering in electric-dipole excitations of  $^6\text{Li}$ ", Phys. Rev. C **100**, 024334 (2019)
- [6] S.A. Rakityansky, N. Elander, "Analytic structure of the multichannel Jost matrix for potentials with Coulombic tails", Journal of Mathematical Physics, **54**, 122112 (2013)
- [7] S.A. Rakityansky and S.N. Ershov, "Jost-matrix analysis of the resonance  $^5\text{He}^*(\frac{3}{2}^+)$  near the  $dt$ -threshold", International Journal of Modern Physics, **E28** (8), 1950064 (37 pages) (2019)
- [8] S.A. Rakityansky, S.N. Ershov, T.J. Tshipi, "Resonance states  $0^+$  of the Boron isotope  $^8\text{B}$  from the Jost-matrix analysis of experimental data", International Journal of Modern Physics, **E28** (8), 1950083 (21 pages) (2019)
- [9] P. Vaandrager, S.A. Rakityansky, "Residues of the  $S$ -matrix for several  $\alpha^{12}\text{C}$  resonances from the Jost function analysis", Nucl. Phys. A **992**, 121627(2019)
- [10] B. Jenny, W. Gruebler, V. König, P. A. Schmelzbach, C. Schweizer, "Phase-Shift Analysis of  $d$ - Elastic Scattering Between 3 and 43 Mev", Nuc. Phys. A **397**, pp. 61-101 (1983)
- [11] V. M. Krasnopol'sky, V. I. Kukulin, E. V. Kuznetsova, "Energy-dependent phase-shift analysis of  $^2\text{H} + ^4\text{He}$  scattering in the energy range  $0.87 < E_d < 5.24 \text{ MeV}$ ", Phys. Rev. C **43**(2), pp. 822-834 (1991)

- [12] P. Vaandrager and S. A. Rakityansky, “*Extracting the resonance parameters from experimental data on scattering of charged particles*”, *Int. J. Mod. Phys. E* **25**, 1650014(2016)
- [13] F. James and M. Roos, “*Minuit - a system for function minimization and analysis of the parameter errors and correlations*”, *Comp. Phys. Comm.* 10 (1975) 343-367; <http://hep.fi.infn.it/minuit.pdf>
- [14] S.A. Rakityansky, N. Elander, “*A method for extracting the resonance parameters from experimental cross section*”, *Int. J. Mod. Phys. E* **22**(5), 1350032(2013)